Proceedings of the Korean Nuclear Society Spring Meeting
Cheju, Korea, May 2001

A CONTROL-VOLUME APPROACH FOR THREE-DIMENSIONAL NUCLIDE TRANSPORT AROUND A GEOLOGICAL REPOSITORY

Y.M. Lee*, Y.S. Hwang, C.H. Kang, S.G. Kim, K.W. Han
Korea Atomic Energy Research Institute, Taejon 300-600, Korea
*e-mail: ymlee@kaeri.re.kr

Abstract

Adopting the control-volume finite difference method, a three-dimensional numerical model for nuclide transport of an arbitrary length of decay chain in a buffer between a canister and an adjacent rock in a high-level radioactive waste repository is proposed. Assuming a linear sorption isotherm, nuclide transport due to diffusion in a buffer and a rock matrix, and advection and dispersion along thin rigid parallel fractures existing in a saturated porous rock matrix as well as diffusion through the fracture wall into the matrix is considered. To illustrate the model, three-dimensional volume plots of concentration isopleths are shown for a typical case with ^{234}U.

Notation

$2b$ = fracture aperture, [L]
b = super- and subscripts denoting the buffer
b,p = super- and scripts denoting the buffer and the matrix together
$\tilde{c}_l(t)$ = concentration of nuclide l at the inlet, [ML^{-3}]
c_E, c_W, c_N, c_S, c_F, c_B c_P = concentrations at each grid point as shown in Figs. 4 and 5, [ML^{-3}]
c_l = concentration of nuclide l, [ML^{-3}]
c_l^0 = initial concentration of nuclide l at the inlet, [ML^{-3}]
D^* = molecular diffusion coefficient in water, [L^2T^{-1}]
$D_{b®f}$ = interface diffusion coefficient through the buffer-fracture interface, [L^2T^{-1}]
$D_{b®p}$ = interface diffusion coefficient through the buffer-matrix interface, [L^2T^{-1}]
$D_{f®p}$ = interface diffusion coefficient through the fracture-matrix interface, [L^2T^{-1}]
D_L = longitudinal hydrodynamic dispersion coefficient in the fracture, further expressed as $D_L = \alpha_L \cdot v + D^*$, [$L^2T^{-1}$]
D_{ty}, D_{tz} = transverse hydrodynamic dispersion coefficients in the fracture in the y- and z-direction, respectively, [L^2T^{-1}]
e, w, n, s, f, b = control volume faces as defined in Figs. 4 and 5
E, W, N, S, F, B, P = subscripts for grid point concentration as shown in Figs. 4 and 5
f = super- and subscripts denoting the fracture

J_w, J_e = total fluxes in the fracture across control volume faces w and e, respectively as shown in Fig. 5(a), [$ML^{-2}T^{-1}$]
l = subscript denoting parent nuclide
l-1 = subscript denoting daughter nuclide
p = super- and subscripts denoting the matrix
R_l = retardation coefficient in the fracture for nuclide l
R_l^b = retardation coefficient in the buffer for nuclide l
R_l^p = retardation coefficient in the matrix for nuclide l
t = elapsed time, [T]
$t_{0.5}$ = half-life of nuclide, [T]
v = groundwater velocity in the fracture, [LT^{-1}]
x, y, z = coordinates as defined in Fig. 1, [L]
x_c = radius of canister (see Fig. 2), [L]
x_b = outer radius of buffer region (x_b - x_c = buffer thickness), [L]
x_L, y_L = distances to the outlet boundary in the x- and y-direction, respectively, [L]
α_L = dispersivity along the fracture, [L]
$(\delta x)_e$, $(\delta x)_w$, $(\delta y)_s$, $(\delta y)_n$, $(\delta z)_f$, $(\delta z)_b$ = distances between nodes as defined in Fig. 5(b), [L]
$(\delta x)_{e+}$ = distance as defined in Fig. 5(b), [L]
Δx_i, Δy_j, Δz_k = spatial discretization increment in the x-, y-, and z-direction, respectively [L]
Δt = temporal increment, [T]
λ_l = decay constant of nuclide l, [T^{-1}]
θ_b = porosity of the buffer
θ_f = porosity of the fracture set to 1.0
θ_p = porosity of the matrix
$(\theta_b D_x^b)$, $(\theta_b D_y^b)$, $(\theta_b D_z^b)$ = effective diffusion coefficients in the buffer in the x- and y-, and z-direction, respectively, [L^2T^{-1}]
$(\theta_p D_x^p)$, $(\theta_p D_y^p)$, $(\theta_p D_z^p)$ = effective diffusion coefficients in the matrix in the x-and y-, and z-direction, respectively, [L^2T^{-1}]

Introduction

In Korea, like many other countries, a potential repository for the final disposal of high-level radioactive waste (HLW) is to be located in a deep geological formation. The disposal concept for the repository would be similar to that of the Swedish KBS-3 (1983) concept. In this concept spent fuel assemblies in canisters individually emplaced in vertical deposition holes. The buffer material, having low permeability, is designed to delay the contact of the waste by groundwater and to have strong sorption capacity to retard or to delay the release of nuclides to such geologic media as host rocks.
Therefore it is important to study the nuclide release through a buffer material into a rock for the radiological safety assessment. For an HLW repository located in deep geological formations, behavior of chain decaying nuclides in geological media has been an important topic in assessing its performance.
However, unfortunately, only a limited number of analytical works for limited modeling system are available for the multi-member chain decay transport. To overcome limitations associated with analytical models, many numerical approaches have been developed for decades (*e.g.*, Grisak and Pickens, 1980; Huyakorn *et al*., 1983a; Lee *et al*., 1989; Kennedy

and Lennox, 1995). However, many of these do not exactly model the migration behaviors or decay chains of an arbitrary length, which is essential in analysis of radioactive waste disposal systems. As for the decay chain models, although Sudicky and Frind (1984) attempted to derive an exact analytical solution for two-member decay chain transport in a fractured medium, neglecting hydrodynamic dispersion along the fracture, a complete analytical solution in a closed form may not yet available for multi-member chain decay and transport, whereas many solutions for a porous medium without matrix diffusion or for the media having a rather simple geometry have been found in the literature (e.g., Harada *et al*., 1980; Lung, 1986; Gureghian, 1987; Kang, 1989).

Since Huyakorn *et al*. (1983b) dealt with decay chain transport in a fractured porous medium by utilizing a finite element technique, various different kinds of numerical scheme have been introduced (e.g. Yamashita and Kimura, 1990 ; Lee and Lee, 1995).

Recently a series of studies associated with chain decay transport have been done numerically by authors (Lee et al., 1993; Lee et al., 1995; Lee and Lee, 1995; Lee et al, 1996; Lee and Kang, 1997; Lee et al, 1997).

Also, a two-dimensional finite-difference numerical solution for nuclide transport of an ‘arbitrary decay chain length’ (i.e., multi-member chain decay) through a buffer and an adjacent fractured porous medium by a control volume method has been developed and the exactness of this solution by comparisons with available analytical solutions has been investigated in a series of works by Lee and Kang (1999a; 1999b) and Lee et al. (1999).

The purpose of this paper is to extend the previous work by considering the media as a three-dimensional modeling domain and to visualize how nuclides transport across a buffer-matrix and buffer-fracture interfaces around a canister, even though the work has not completely done yet.

Conceptual Model

Nuclides escaped from a penetrated canister diffuse eventually to the host rock through a buffer material. Fractures in a host rock of a geological repository around a canister intersect disposal holes, providing advective pathways for the hydrogeologic nuclide transport, whereas porous rock matrix inerfaced with buffer provides diffusive transport pathways for nuclides. Since fractures having permeabilities several orders of magnitude higher than the rock matrix itself provide a main hydrogeologic pathway for the transport of the nuclide into a far-field region, the assumption that the rock matrix surrounding the buffer is impervious to nuclide transport has commonly been made. However, recently, studies show that nuclides are available to diffuse freely across the buffer-matrix boundary. Such an approach is difficult to be handled with an analytical method due to the complexity of a domain.

The physical system of a fractured rock modeled here is similar to that treated in many works (e.g., Sudicky and Frind, 1982; Sudicky and Frind, 1984; Lee et al., 1989; Lee et al., 1993; Lee, 1995; Lee and Lee, 1995; Lee and Kang, 1997). In these models thin rigid parallel fractures are embedded in a saturated porous rock matrix. The buffer is modeled as a three-dimensional porous medium as shown in Fig. 1. The geometry and the dimension of the modeled domain are also shown in Fig. 2.

If a linear sorption isotherm is assumed, transport for the nuclide l in a saturated fracture is commonly described by

$$R_l \frac{\partial c_l}{\partial t} + \lambda_l c_l R_l = \frac{\partial}{\partial x}\left(D_L \frac{\partial c_l}{\partial x} - v c_l \right) + \frac{\partial}{\partial y}\left(D_{ty} \frac{\partial c_l}{\partial y} \right) + \frac{\partial}{\partial z}\left(D_{tz} \frac{\partial c_l}{\partial z} \right) + \lambda_{l-1} c_{l-1} R_{l-1}, \quad (1)$$
$$x_b \cos\phi \le x \le x_L \left(0 \le \phi \le \pi/2\right), 0 \le y \le b, 0 \le z \le x_b, t > 0.$$

Also, assuming that there is no advective transport in the buffer as well as in the matrix, the governing equation is

$$R_l^{b,p} \frac{\partial c_l}{\partial t} + \lambda_l c_l R_l^{b,p} = \frac{\partial}{\partial x}\left(\theta_{b,p} D_x^{b,p} \frac{\partial c_l}{\partial x} \right) + \frac{\partial}{\partial y}\left(\theta_{b,p} D_y^{b,p} \frac{\partial c_l}{\partial y} \right) + \frac{\partial}{\partial z}\left(\theta_{b,p} D_z^{b,p} \frac{\partial c_l}{\partial z} \right) + \lambda_{l-1} c_{l-1} R_{l-1}^{b,p},$$
$$\begin{cases} x_c \cos\phi < x < x_b \cos\phi, 0 < y < y_L, x_c \sin\phi < z < x_b \sin\phi, t > 0; & \text{for bufffer} \\ x_b \cos\phi < x < x_L, b < y < y_L, x_b \sin\phi < z < x_b \sin\phi, t > 0; & \text{for matrix.} \end{cases} \quad (2)$$

The discretized domain a the buffer and a fractured porous media is depicted in Fig. 3, where the boundary conditions are zero concentration gradient (Neuman-type) boundary conditions at all boundaries except one at the canister surface interface, *i.e.*,

for the inlet and the outlet of the modeled domain the *y*-*z* plane:

$$\frac{\partial c_l}{\partial x} = 0, \quad x = 0, 0 \le y \le y_{L,}\, x_c \le z \le x_b \text{ and } x = x_L; \quad (3a)$$

at the lower boundary of a buffer ($y = 0$) and at centers of a fracture and a matrix between two parallel fractures (*x*-*z* plane):

$$\frac{\partial c_l}{\partial y} = 0; \quad x_c \cos\phi \le x \le x_L\, 0 \le z \le x_b, \begin{cases} y = 0, \text{and} \\ y = y_L \end{cases}; \quad (3b)$$

and finally for the *x*-*y* plane:

$$\frac{\partial c_l}{\partial z} = 0; \quad 0 \le y \le y_L, \begin{cases} z = 0, x_c \le x \le x_L, \text{and} \\ z = x_b, 0 \le x \le x_L \end{cases} \quad (3c)$$

For initial and boundary conditions associated with the inlet of a buffer, nuclide decay and transformation of a parent nuclide into its daughter are considered together by the Bateman's decaying source. Therefore the concentration at the inlet boundary for the *l*-th component of the decay chain, $\tilde{c}_l(t)$ is written as

$$\tilde{c}_l(t) = \sum_{m=1}^{l} B_{lm} e^{-\lambda_m t} \quad (4a)$$

where

$$B_{lm} = \sum_{n=1}^{m} c_n^0 \prod_{k=n}^{l-1} \lambda_k \left\{ \prod_{\substack{j=n \\ j \ne m}}^{l} \left(\lambda_j - \lambda_m\right) \right\}^{-1} \quad (4b)$$

and c_l^0 denotes the initial concentration due to an inventory at the inlet.

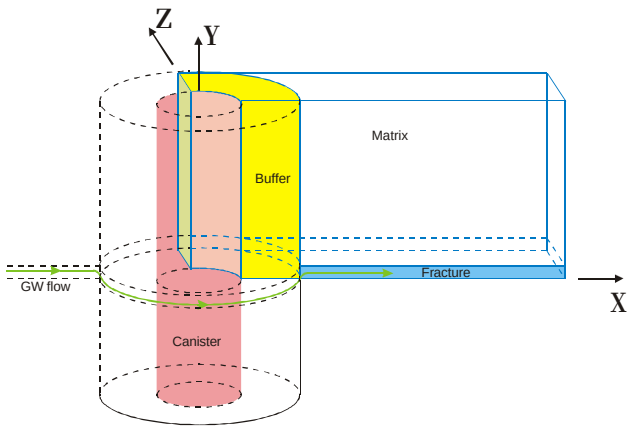

3d_domain.cdr

Fig. 1. Schematic view in the vicinity of a deposition hole intersected by a fracture in a potential HLW repository tunnel.

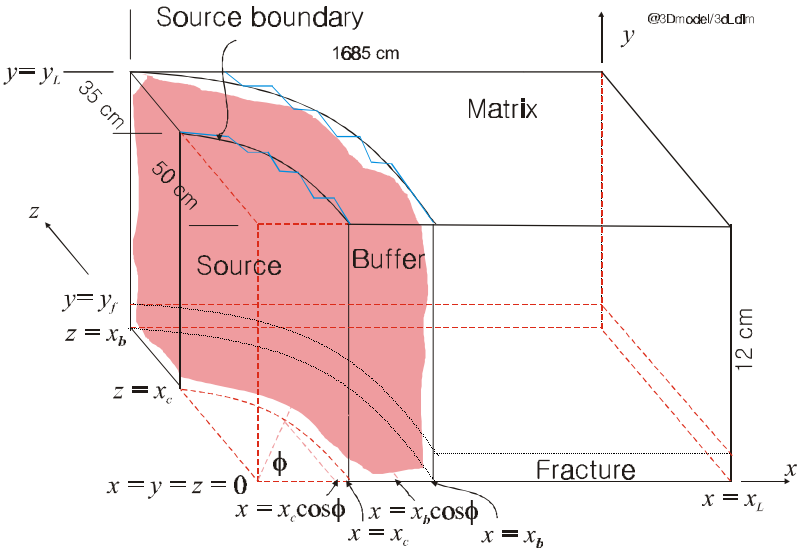

Fig. 2. The dimension of the modeled domain.

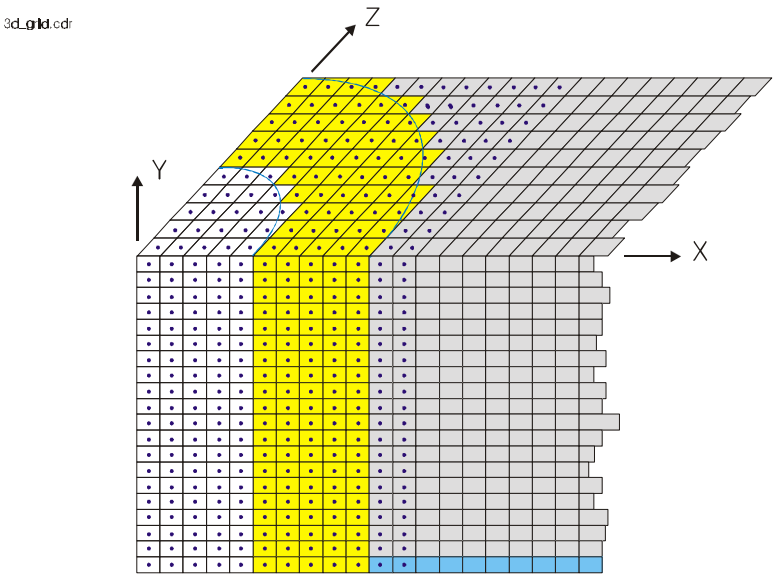

Fig. 3. Three-dimensional discretization concept of the domain.

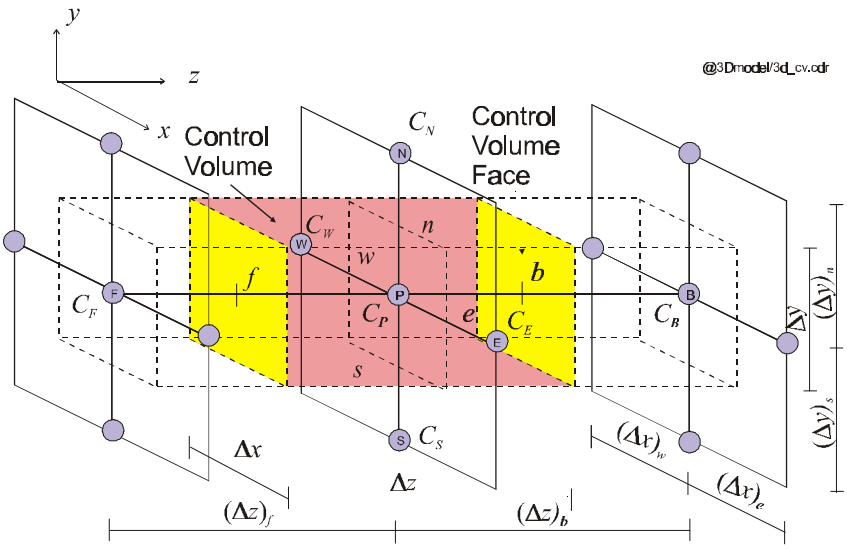

Fig. 4. A control volume and notations.

To derive a three-dimensional discretization equation by the control volume approach, first of all, a grid-point cluster is introduced. (See Figs. 3 and 4.) The modeled domain is divided into variably sized control volumes, each of which has a central grid point, *P* located in the geometrical center of the control volume. The control volume faces are not necessarily located equidistant from the each adjacent node. Once the control volumes have been defined, the concentration value is evaluated at each node.

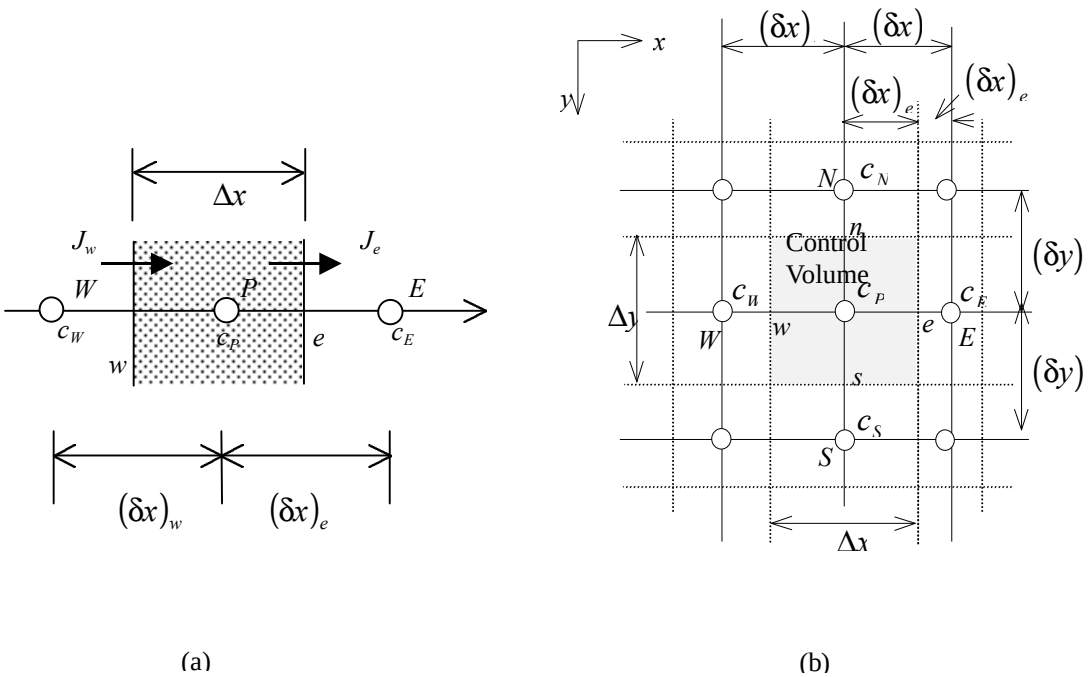

(a) (b)

Fig. 5. (a) Steady state one-dimensional consideration for the flux in the fracture (in the *x*-direction); (b) Two-dimensional view of control volume in the *x*-*y* plane.

In order to avoid a discontinuity in physical properties within a control volume, discontinuities in the medium, such as at the no flux boundary and the fracture-matrix boundary, are recommended to be located at control volume faces. Although it leads to the half-sized control volumes around the grid points, by postulating a grid point at the face having control volume of zero thickness, the need for special discretization at discontinuities can be eliminated.

Numerical Illustration

Even though any works associated with demonstration of the validity and relative accuracy of the scheme developed in this study has not carried out, several examples limited to two-dimensional work for the fractured rock medium without consideration of the buffer medium have been considered in comparisons with available analytical solutions through the previous works (Lee and Kang, 1999a). No further verification for current three-dimensional model are not made in this study.

Table 1. Spatial increments for the control volume

Dx_i, cm i = 1, 2, 3, …, 100	7 (i=1~5), 10 (i=6~10), 15 (i=11~50), 20 (i=51~100)
Dy_j, cm j = 1, 2, 3, …, 20	0.006 (=b/2), 0.009, 0.015, 0.025, 0.045, 0.07, 0.13, 0.25, 0.45, 1 (j=10~20)
Dz_k, cm j = 1, 2, 3, …, 10	7 (k=1~5), 10 (k=6~10)

As seen in the Table 1, the number of control volumes used is 100 along the fracture axis in the x-direction, 20 in the y-direction into the matrix, and 10 in the horizontal z-direction, giving a total of $100 \times 20 \times 10$ control volumes.
Parameters used are also listed in Tables 2 and 3.

Table 2. Nuclide data for ^{234}U.

Nuclide	$t_{0.5}$, yr	R_l, R^b_l, R^p_l	c_l^0
^{234}U	2.47×10^5	0	$c_0 = 1.0$

The volume plots of concentrations of ^{234}U in the media around the quartile section of a canister, normalized to the parent nuclide (^{234}U) concentration at the inlet boundary surface of the canister where $\tilde{c}_l$ is decayed time-dependently according to Bateman equation (Eqs. (4) and (6) in Table 4), as a function of distances in the x-, y- and z-directions at time equal to 1×10^6 years are shown in Figs. 6 and 7. Fig. 6 shows the isopleths in case there are no matrix diffusions both from the buffer and the fracture are considered. On the other hand, Fig. 7 shows the case when all matrix diffusion are involved.
^{234}U has the decay chain of $^{234}\text{U} \rightarrow {}^{230}\text{Th} \rightarrow {}^{226}\text{Ra} \rightarrow \cdots\cdots$, which is one of the most important one in HLW. It is emphasized that the solution and the associated computer code developed in this study are not limited by the specific number of members in the chain.
With the advection-dispersion parameters chosen, the result visualizes the isopleths that ^{234}U travels physically well around a canister, a buffer and other surrounding media.

Table 3. Parameters used

Parameter	Value
$2b$	120 μm
θ_b	0.1
θ_f	1.0
θ_p	0.4
α_L	0.76 m
v	0.75 m/yr
$(\theta D_x^p) = (\theta D_y^p) = D^*$	8.64×10^{-6} m^2/yr
D_L	$\alpha_L \cdot v + D^*$
x_c	35cm
x_b	85cm
x_L	16.85m
y_L	12cm
z_L	85cm

Table 4. Initial and boundary conditions for illustration

I.C.	$c_l(x, y, z; t = 0) = 0$, l = 1, 2, 3 (5)
B.C. (@ inlet)	$c_l(x = x_c \cos\phi, 0 \le y \le y_L, 0 \le z \le x_b; t) = \tilde{c}_l$, l = 1, 2, 3, … (6a) $vc_l(x = x_c \cos\phi, 0 \le y \le y_L, 0 \le z \le x_b; t) - D_L \frac{\partial c_l}{\partial y} = v\tilde{c}_l$, l = 1, 2, 3, … (6b)

For more effective calculation, varying temporal steps according to the calculation time can be used. After some numerical experiments through a series of the previous works associated with the control volume discretization, optimum temporal sizes have been obtained, even though the results are not shown again in this paper. Among these values some acceptable time steps are chosen.

To deal with interface diffusion coefficients, $D_{f®p}$, $D_{b\to p}$, and $D_{b\to f}$ when the diffusion coefficients or dispersion coefficients are different in adjacent control volumes as in such cases as the fracture wall interfaced with the matrix and the buffer interfaced with rock, the analogy to a series of resistors can be utilized in the same way as discussed by Patankar (1980).

The same values of retardation factors for each medium of a buffer, a matrix and a fracture are used for simplicity, which does not seem to affect any illustrative purpose addressed by this study.

By investigating two different cases, very naturally, it is shown that ^{234}U in Fig. 6 travels faster than ^{234}U in Fig. 7. This is due to the fact that nuclides entering a fracture are taken away by advection and dispersion due to groundwater flow takes place only in the fracture although there is no loss term due to matrix diffusion into a matrix from a fracture unlike the case depicted in Fig. 7. Also, no nuclides are supplied from a buffer into a rock except through the inlet of a fracture.

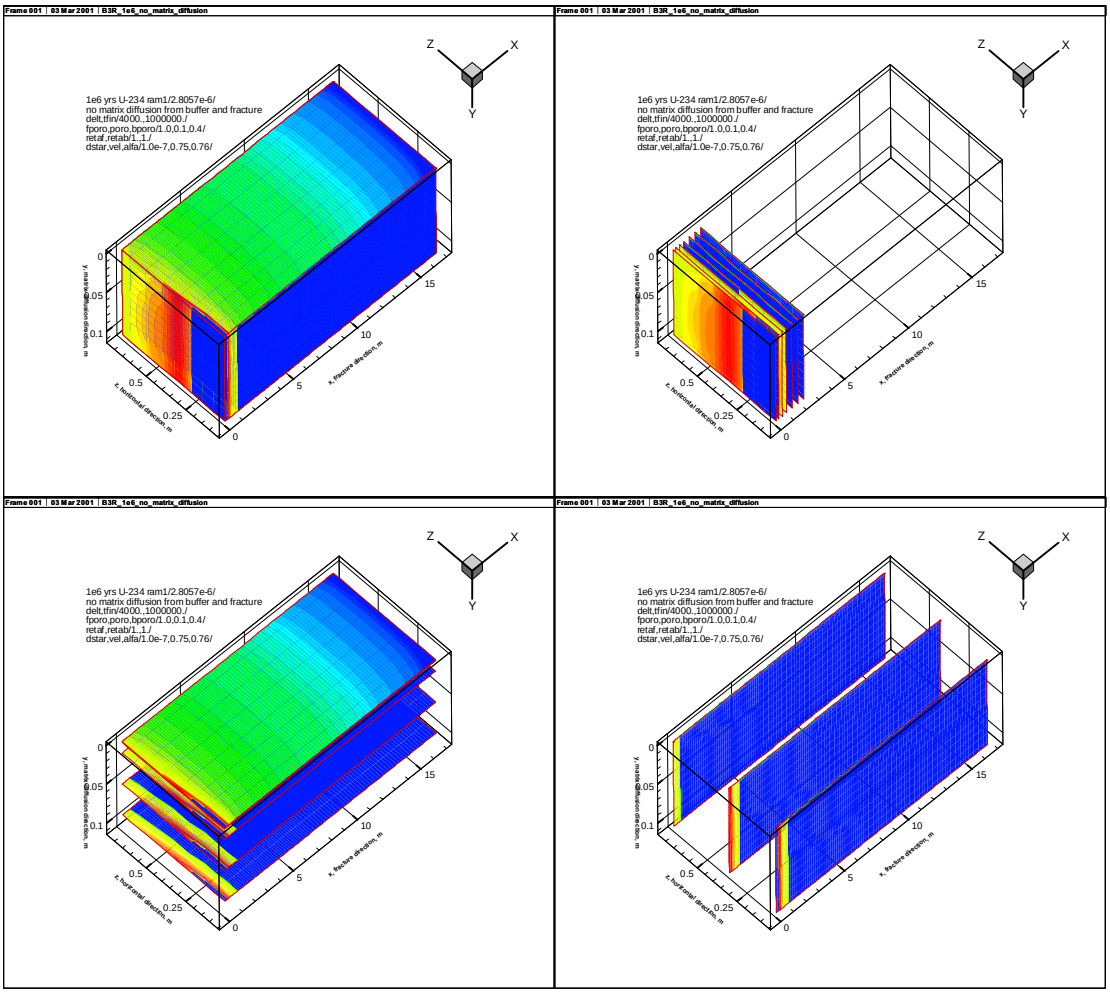

Fig. 6. Volume plot for ^{234}U at time of 1×10^6 years (no matrix diffusion from buffer and matrix).

Concluding Remarks

A three-dimensional model has been introduced for multi-member chain decay and transport through a fractured porous rock matrix. For demonstration, only a mother nuclide ^{234}U is used in numerical examples.

The model is based on a physically exact formulation by utilizing a control volume method and then the differential governing equation is directly integrated over each control volume. This study is an extension of previous work by Lee and Kang (1999a; 1999b) who developed the two-dimensional model for decay chain transport in a composite media of a buffer and a fractured porous medium.

This kind of work is considered to be useful especially when a visualization is needed to represent the nuclide behavior around the canister and there needs a graphical representation of the nuclide transport behavior around the deep geological repository to investigate transport phenomena through a geologic medium to demonstrate the safety of a repository.

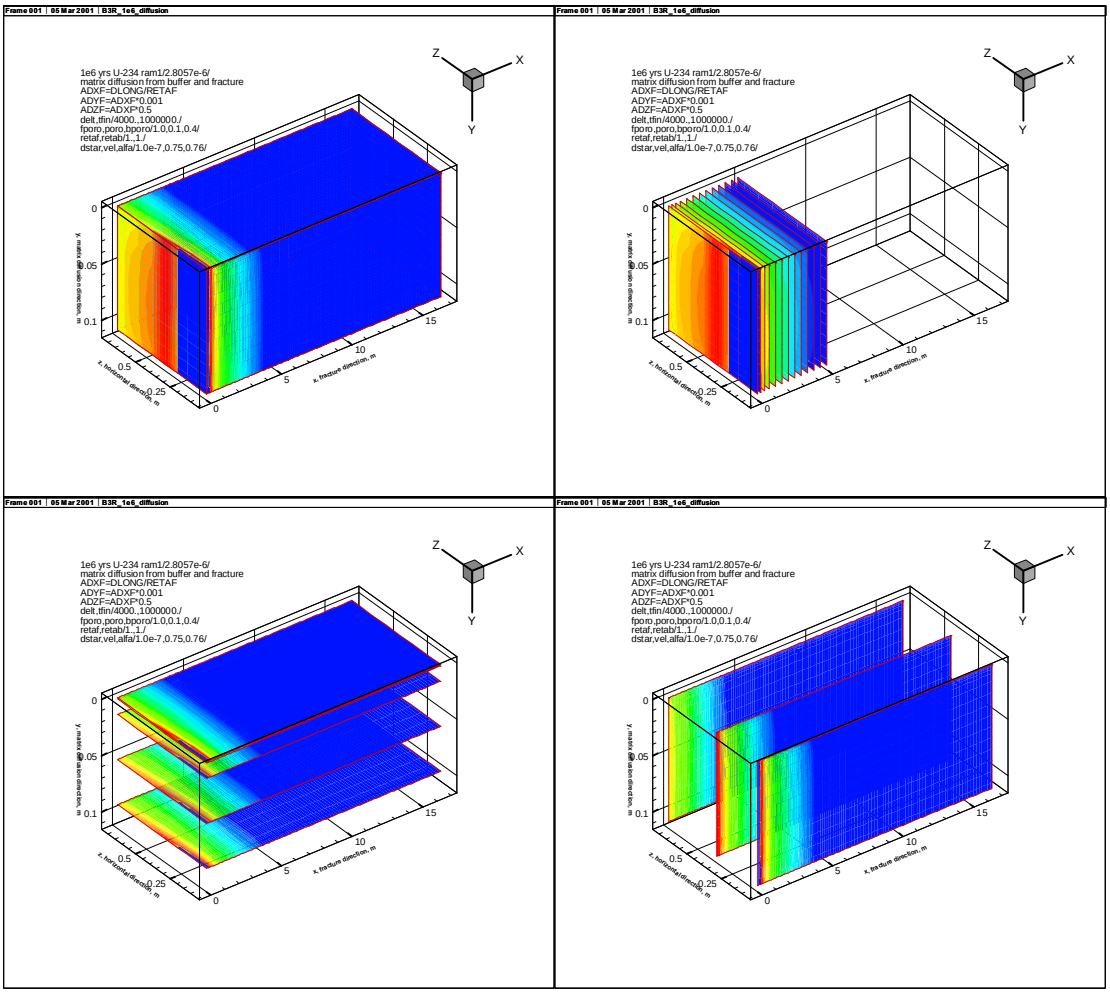

Fig. 7. Volume plot for ^{234}U at time of 1×10^6 years (with matrix diffusion from buffer and matrix together).

References

Grisak, G.E. and J.F. Pickens, *Water Resour. Res*., **16**(4), 719, (1980).

Gureghian, A.B., BMI/OCRD-25, (1987).

Harada et al., ONWI-359, LBL-10500, UC-70, (1980).

Huyakorn, P.S. *et al*., *Water Resour. Res*., **19**(3) 841, (1983a).

Huyakorn, P.S. *et al*., *Water Resour. Res*., **19**(5) 1286, (1983b).

Kang, C.H., Ph.D. Thesis, Chapter 2, U.C.-Berkeley, (1989).

Kennedy C.A. and W.C. Lennox, *Water Resour. Res*., **31**(2) 313, (1995).
Lee Y.M., Ph.D. Thesis, Chapter 5, KAIST, (1995).

Lee Y.M. *et al*., *J. Korean Nucl. Soc*., **21**(4), 267, (1989).

Lee, Y.M et al., *J. Korean Nucl. Soc,* **31**(4), 432, (1999).

Lee, Y.M. and C.H. Kang, Proc. MRS'97, Sept. 28-Oct. 3, 1997, Davos, Switzerland, (1997).

Lee, Y.M. and K.J. Lee, *Ann. Nucl. Energy*, **22**(2), 71, (1995).

Lee, Y.M., et al., *J. Korean Nucl. Soc*., **28**(2), 539, (1996).

Lee, Y.M. et al., *J. Korean Nucl. Soc*., **29**(4), 539, (1997).

Lee, Y.M., et al., *J. Korean Nucl. Soc*., **25**(4), 539, (1993).

Lee, Y.M., et al., *J. Korean Nucl. Soc.,* **21**(4), 267, (1989).

Lee, Y.M., et al., Proc. of WM95, February 26 - March 2, 1995, Tucson, Arizona, U.S.A., (1995).

Lee, Y.M. and C.H. Kang, *Annals of Nuclear Energy*, **26**(17), 1569, (1999a).

Lee, Y.M. and C.H. Kang, Proc. Migration '99, Sept, 26-Oct. 1, 1999, Incline Village, Nevada/California, U.S.A., (1999b).

Lung, H.-C., Ph.D. Thesis, Chapter 5, University of California-Berkeley, (1986).

Patankar, S.V., Numerical Heat Transfer and Fluid Flow, Hemisphere, Washington, D.C., (1980).

Sudicky, E.A. and E.O. Frind, *Water Resour. Res*., **18**(6), 1634, (1982).

Sudicky, E.A. and E.O. Frind, *Water Resour. Res*., **20**(7), 1021, (1984).

Yamashita R. and H. Kimura, *J. Nucl. Sci. Tech*., **27**(11), 1041, (1990).